Data Based Color Constancy

Wei Xu, Huaxin Xiao, Yu Liu and Maojun Zhang
College of Information System and Management, National University of Defense Technology, Changsha, China

Keywords: Color Constancy, Color Gamut, Canonical Illuminant, Data Driven, Kernel Method.

Abstract: Color constancy is an important task in computer vision. By analyzing the image formation model, color gamut data under one light source can be mapped to a hyperplane whose normal vector is only determined by its light source. Thus, the canonical light source is represented through the kernel method, which trains the color data. When an image is captured under an unknown illuminant, the image-corrected matrix is obtained through optimization. After being mapped to the high-dimensional space, the corrected color data are best fit for the hyperplane of the canonical illuminant. The proposed unsupervised feature-mining kernel method only depends on the color data without any other information. The experiments on the standard test datasets show that the proposed method achieves comparable performance with other state-of-the-art methods.

1 INTRODUCTION

Under different color light sources, objects present different colors. Human eyes can automatically adapt to the light changes that retain the perception of object color. This phenomenon is known as color constancy. However, given the limitation of image sensors, the image captured by digital imaging devices does not have color constancy. Color is one of the most important features of vision. Many computer vision applications need color information, such as image segment (Zhuang et al., 2012), object recognition and tracking (Bousetouane et al., 2013), and image retrieval (Stottinger et al., 2012). The object color variation caused by a light source influences the robustness of the above algorithms. Thus, the color constancy algorithm is important in computer vision.

Many color constancy methods have been proposed in the past decades. Some of these methods directly set constraints or assumptions on the scene, such as Grey World (Buchsbaum, 1980), White Patch (Land, 1977), Shades of Grey (Finlayson and Trezzi, 2004), Grey Edge (van de Weijer et al., 2007), Grey Block-Differencing (Lai et al., 2013), and Gamut Mapping (Forsyth, 1990; Gijsenij et al., 2010). Other methods seek light source-related prior information by machine learning to predict the unknown illuminant. Cardei et al. (Cardei et al., 2002) employed the Neural Network method. Although this method seems to be a reasonable solution, it lacks a detailed description of the problem. In practice, its generalization ability is poor. Bayesian statistical theory (Brainard and Freeman, 1997; Finlayson et al., 2001; Rosenberg et al., 2004; Gehler et al., 2008) is also commonly used, which determines the specific probability distribution as prior knowledge. However, accurately describing this distribution is difficult. Funt et al. (Funt and Xiong, 2004) used Support Vector Regression (SVR). Their training set consists of the binarized chromaticity histograms of many images. Chakrabarti et al. (Chakrabarti et al., 2008; Chakrabarti et al., 2012) attempted to develop a statistical model for the spatial correlations between pixels.

In this study, we examine the color gamut data from a new perspective. By analyzing the image formation model, the color gamut data can be mapped to a hyperplane whose normal vector is determined by the light source. This hyperplane unifies the disorderly color gamut data. Thus, the color data captured under the canonical illuminant are trained to implicitly obtain the features of the canonical light source. The training method is an unsupervised feature mining kernel method, such as SVR, which is a supervised method. Our algorithm uses the entire color gamut during training, which is different from the gamut mapping method (Finlayson et al., 1993) that uses the data only on the convex hull. When correcting an image under an unknown illuminant, the corrected matrix is computed by optimization. The color data of the corrected image can be best fit for the hyperplane of the canonical illuminant after mapping to a high-dimensional space. Considering that this method only depends on the color data without any

Xu, W., Xiao, H., Liu, Y. and Zhang, M.
Data Based Color Constancy.
DOI: 10.5220/0005698104310436
In *Proceedings of the 5th International Conference on Pattern Recognition Applications and Methods (ICPRAM 2016)*, pages 431-436
ISBN: 978-989-758-173-1

other information, it is called the data-driven color constancy method in this study.

The rest of this paper is organized as follows. Section 2 presents our algorithm, which consists of analysing the image formation model. Section 3 tests our method on the standard test datasets and discusses the results. Finally, Section 4 summarizes this work and discusses future research.

2 PROPOSED METHOD

2.1 Analysis of the Color Gamut Data

Similar to most color constancy algorithms, we assume that the scene only has one light source and the object reflection is diffusion, which conforms to the ideal Lambertian model (Barnard, 1999). According to the Lambertian reflection model, image formation depends on three factors: the light source $L(\lambda)$, surface reflectance properties $S(x,\lambda)$, and camera sensitivity $\mathbf{C}(\lambda)$. Thus:

$$\boldsymbol{\rho}^{\mu}(x) = \int_{\omega} S(x,\lambda)L(\lambda)\mathbf{C}(\lambda)\mathrm{d}\lambda, \tag{1}$$

where x is the spatial coordinate of the image; λ is the spectrum wavelength; ω is the visible wavelength range; $\mathbf{C}(\lambda) = [C_r(\lambda), C_g(\lambda), C_b(\lambda)]^T$ is the spectrum response function of the camera for the three color bands (i.e., red, green, and blue); and $\boldsymbol{\rho}^{\mu}(x)$ is the RGB value at point x under the unknown illuminant, namely, $\boldsymbol{\rho}^{\mu}(x) = [\rho_r^{\mu}(x), \rho_g^{\mu}(x), \rho_b^{\mu}(x)]^T$.

The aim of color constancy is to adjust the image obtained under an unknown illuminant to the canonical illuminant, as shown in the following equation:

$$\boldsymbol{\rho}^{c}(x) = \Lambda^{\mu,c}\boldsymbol{\rho}^{\mu}(x). \tag{2}$$

where $\boldsymbol{\rho}^{c}(x)$ is the image in the canonical illuminant and Λ is a constant diagonal matrix (Finlayson et al., 1993).

Based on a previous study (F.-H. Cheng and Chen, 1998), spectral power distribution can be expressed as follows:

$$L(\lambda) = \sum_{i=1}^{n} e_i E_i(\lambda), \tag{3}$$

where $E_i(\lambda)$ is the basis function used to describe the spectral power distributions of illuminants, e_i is the corresponding weight, and n is the number of basis functions. Substituting $L(\lambda)$ in Equation (1) with Equation (4) yields the following:

$$\boldsymbol{\rho}(x) = \sum_{i=1}^{n} \big(e_i \int_{\omega} E_i(\lambda)S(x,\lambda)\mathbf{C}(\lambda)\mathrm{d}\lambda\big). \tag{4}$$

For each component of $\boldsymbol{\rho}(x)$, the following equation is derived:

$$1 = \sum_{i=1}^{n} \big(e_i \int_{\omega} \frac{E_i(\lambda)S(x,\lambda)C_k(\lambda)}{\rho_k(x)}\mathrm{d}\lambda\big). \tag{5}$$

where $k = r,g,b$.

Summing up the red, green, and blue components yields the following:

$$-\Big(\sum_{i=1}^{n} \big(e_i \int_{\omega} \sum_{k=r,g,b} \frac{E_i(\lambda)S(x,\lambda)C_k(\lambda)}{3\rho_k(x)}\mathrm{d}\lambda\big)\Big) + 1 = 0. \tag{6}$$

It can be abbreviated in hyperplane form as follows:

$$< \mathbf{w}, \chi > +1 = 0, \tag{7}$$

where $< \cdot, \cdot >$ is the inner product, $\mathbf{w} = [e_1, e_2, \cdots, e_n]$, and $\chi = \Big[-\big[\int_{\omega}\sum_{k=r,g,b}\frac{E_i(\lambda)S(x,\lambda)C_k(\lambda)}{3\rho_k(x)}\mathrm{d}\lambda\big]_{i=1}^{n}\Big]^T$. The function Φ that can map the color gamut data to the n-dimensional space H is then defined. If it satisfies:

$$\Phi([\rho_r(x), \rho_g(x), \rho_b(x)]) = -\Big[\int_{\omega}\sum_{k=r,g,b}\frac{E_i(\lambda)S(x,\lambda)C_k(\lambda)}{3\rho_k(x)}\mathrm{d}\lambda\Big]_{i=1}^{n}, \forall x, \tag{8}$$

any pixel in the image can project to the hyperplane, which is determined by the normal vector $\mathbf{w}$. The normal vector $\mathbf{w}$ is only related to the illuminant parameter e_i, which represent the light source characteristics

2.2 Estimation of Illuminant Parameters

Suppose the color gamut of the known canonical illuminant c is $\Omega^c = \{\boldsymbol{\rho}^c(i)\}_{i=1,2,\cdots,P}$, where P is the number of data in the color gamut, and $\boldsymbol{\rho}^c(i)$ is the RGB value of some data i. After mapping the function Φ, the new data $\chi_i^c = \Phi(\boldsymbol{\rho}^c(i))$ satisfy the corresponding hyperplane Γ^c of the light source. Thus:

$$\Gamma^c :< \mathbf{w}^c, \chi_i^c > +1 = 0, \tag{9}$$

where normal vector $\mathbf{w}^c$ is the illuminant characteristic.

The kernel function can denote the inner product of the high-dimensional space in the original low-dimensional space, i.e., $K(a,b) =< \Phi(a), \Phi(b) >$. Thus, the kernel function is employed to approximate Φ.

Similar to the derivation of SVR, the loss function $\xi = L(0, < w^c, \chi_i^c > +1)$ is defined. The target is to minimize the total loss as follows:

$$\begin{aligned} w^c &= \arg\min_{w^c} \sum_{i=1}^{P} \xi_i \\ s.t. \quad \xi_i &= L(0, < w^c, \chi_i^c > +1). \end{aligned} \tag{10}$$

The ε-insensitive loss function is used to deal with the noise in the observed data as follows:

$$L(0,< w^c,\chi_i^c > +1) = |< w^c,\chi_i^c > +1|_\varepsilon . \quad (11)$$

In general, the observed data contain noise. Regularization is utilized in controlling the capacity of the function cluster to avoid over-fitting. In particular, the magnitude of $\|w^c\|^2$ is restricted, where $\|\cdot\|$ is a 2-norm operator, and the variable η is used as the weight to leverage the capacity and errors. The problem is then transformed to solve the minimization problem of the optimization objective function as follows:

$$\begin{aligned} w^c \quad &= \quad \arg\min_{w^c} \frac{1}{2}\|w^c\|^2 + \eta\sum_{i=1}^{P}(\xi_i + \widehat{\xi}_i) \quad (12)\\ s.t. \quad &< w^c,\chi_i^c > +1 \le \varepsilon + \xi_i \\ &< w^c,\chi_i^c > +1 \ge -\varepsilon - \widehat{\xi}_i \\ &\xi_i, \widehat{\xi}_i \ge 0, i = 1,2,\cdots,P \end{aligned}$$

where ξ_i and $\widehat{\xi}_i$ are relaxation factors, and the constant $\eta > 0$ indicates the punishment for the excess of the error ε .

By Lagrange duality theory and the introduction of the kernel function, Eq.(12) can be converted to the following quadratic programming problems:

$$\begin{aligned} &(\widehat{\alpha},\alpha) = \\ &\arg\min_{\widehat{\alpha},\alpha} \\ &\frac{1}{2}\sum_{i=1}^{P}\sum_{j=1}^{P}(\widehat{\alpha}_i - \alpha_i)(\widehat{\alpha}_j - \alpha_j)K(\boldsymbol{\rho}^c(i),\boldsymbol{\rho}^c(j)) \\ &+\varepsilon(\sum_{i=1}^{P}(\widehat{\alpha}_i + \alpha_i) + \sum_{i=1}^{P}(\widehat{\alpha}_i - \alpha_i)) \quad (13)\\ &s.t. 0 \le \widehat{\alpha}_i \le \eta \\ &0 \le \alpha_i \le \eta \end{aligned}$$

where $K(\cdot,\cdot)$ is the kernel function. The Gaussian radial basis kernel function $K(a,b) = \exp(-\|a-b\|^2/2(\sigma^2))$ is selected in our method. From the derivation of Eq.(13), the illuminant characteristic can be obtained as follows:

$$\mathbf{w}^c = \sum_{i=1}^{P}(\widehat{\alpha}_i - \alpha_i)\Phi(\boldsymbol{\rho}^c(i)). \quad (14)$$

The illuminant can be implicitly expressed by the parameters $\widehat{\alpha}_i$ and α_i. Although $\mathbf{w}^c$ still relates to the mapping of $\Phi(\boldsymbol{\rho}^c(i)$, the next section discusses that the corrected matrix can be obtained only if $\widehat{\alpha}_i$ and α_i are known.

According to the feature of the support vectors, the obtained $\mathbf{w}^c$ is sparse because of the use of the insensitive loss function. Although $\mathbf{w}^c$ is P - dimensional (i.e., P is the number of data in the color gamut), many zeros exist in $\mathbf{w}^c$. The number of non-zeros is exactly the number of support vectors.

During training, given the large amount of color gamut data (i.e., hundreds of thousands of points), the memory consumption is very large. Thus, we designed an iterative algorithm. In Step 1, 1000 points are uniformly chosen as the subset for training, and their hyperplane is obtained. In Step 2, 150 points that have the maximum distance to the hyperplane are selected and added to the subset to train a new hyperplane. Step 2 is repeated several times to obtain the best hyperplane.

2.3 Estimation of the Corrected Matrix

Given an image $\boldsymbol{\rho}^\mu(x)$ under an unknown illuminant μ, the correction employs the diagonal matrix $\Lambda^{\mu,c} = diag(\mathbf{f})$ according to Eq.2. After the correction, the image color gamut in high-dimensional space can be best fit for the canonical illuminant hyperplane Γ^c. This optimization problem is as follows:

$$\Lambda^{\mu,c} = \frac{\arg\min_{\Lambda^{\mu,c}}\sum_{j=1}^{Q}(< w^c,\Phi(\Lambda^{\mu,c}\boldsymbol{\rho}^\mu(j)) > +1)^2}{\|w^c\|^2}, \quad (15)$$

where $\boldsymbol{\rho}^\mu(j)$ is the RGB value at point j in the unknown illuminant color gamut, and Q is the number of data in the color gamut. When $\Lambda^{\mu,c} = 0$, Eq.15 is clearly degenerated and constantly established. Thus, the constraint is required. In our method, the constraint is $[\Lambda^{\mu,c}]^T\Lambda^{\mu,c} \ge 3$. Its physical meaning is obtained after the correction, and the image brightness remains high. $\Lambda^{\mu,c} = 0$ indicates that the image turns black after the correction. Given that $\mathbf{w}^c$ can be expressed as Eq.14 and $\|w^c\|^2$ is a constant, as shown in the previous section, Eq.15 can be rewritten as follows:

$$\begin{aligned} &\Lambda^{\mu,c} \\ &= \arg\min_{\Lambda^{\mu,c}} \\ &\sum_{j=1}^{Q}\Big(\sum_{i=1}^{P}(\widehat{\alpha}_i - \alpha_i)K\big(\Lambda^{\mu,c}\boldsymbol{\rho}^\mu(j),\boldsymbol{\rho}^c(i)\big) + 1\Big)^2 \\ &s.t. \ [\Lambda^{\mu,c}]^T\Lambda^{\mu,c} \ge 3 \quad (16) \end{aligned}$$

Eq.16 is a nonlinear optimization problem. The damped Gauss−Newton method (Subramanian, 1993; Pan and Chen, 2009) is used to solve this problem, whose convergence is fast and accurate. Approximately 10 iterations are sufficient in our application. More importantly, the global unique solution can be obtained.

3 EXPERIMENTS AND ANALYSIS

Figure 1: Camera used for the SFU Grey-ball dataset collection.

The performance of the proposed algorithm is tested in this section. We primarily performed the experiment on the SFU Grey-ball dataset proposed by Funt et al. (Ciurea and Funt, 2003). This dataset consists of 11,346 consecutive images captured with a video camera. The video contains various indoor and outdoor scenes under different illuminant. The ground truth is captured using a grey sphere mounted on the bottom of the camera (Fig.1), so it is always visible inside the images. Some sample images are shown in Fig.2. The ground truth illuminant of each image and test results of some state-of-the-art methods for the full set are published on the color constancy research website (Gijsenij and Gevers,).

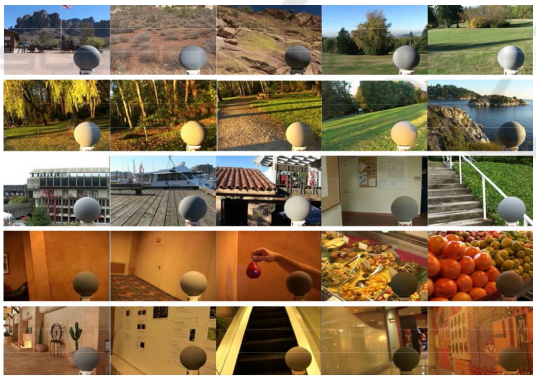

Figure 2: Sample images in the SFU Grey-ball dataset.

The angular error between the estimated illuminant vector $\mathbf{e}^{\varepsilon}$ and the ground truth vector $\mathbf{e}^{i}$ is employed to provide quantitative quality evaluations as follows:

$$e_{arg} = \cos^{-1}\left(\frac{\mathbf{e}^{i} \cdot \mathbf{e}^{\varepsilon}}{\|\mathbf{e}^{i}\| \, \|\mathbf{e}^{\varepsilon}\|}\right) \tag{17}$$

Suppose the corrected matrix $\Lambda^{\mu,c} = diag(l,m,n)$. The estimated illuminant vector $\mathbf{e}^{\varepsilon}$ is computed as $\mathbf{e}^{\varepsilon} = (m/l, 1, m/n)$. Here the quotiety of green component is set to 1. The mean and median angular errors are selected for performance evaluation.

3.1 Experiment Details

We randomly selected 50 images from the training dataset of the canonical illuminant. These images include various scenes under different light sources corrected by the ground truth before training. Based on these images, the color gamut (approximately 40,000 points) of the canonical illuminant can be drawn (Fig.3).

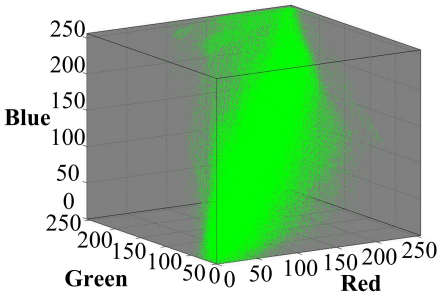

Figure 3: Color gamut of the canonical illuminant.

Three parameters (i.e., λ, ε, and σ) exist in the training process (Eq.(13)). They are empirically set according to their meanings. ε, which is the degree of the tolerance to noise, is set at $\varepsilon = 0.0001$. λ, which is the degree of the punishment for the excess of error ε, is set at $\lambda = 1$. σ, which is the parameter of the Gaussian radial basis kernel, is set at $\sigma = 25$. The run-time of the training takes 20-30 min on our PC (CPU: 3.10 GHZ, OS: Windows 7 64-bit, RAM: 6 GB). Once the illuminant characteristic $\mathbf{w}^{c}$ is obtained, it can be used for the correction of all images.

3.2 Experiment Results

We uniformly selected approximately 1000 images (except the training images) from the dataset to act as the estimation set. The corrected matrix was obtained by the optimization of Eq.(16). Given that the grey ball in the image is used to record the actual illuminant, it needs to be masked to avoid its influence. We uniformly selected 25% of the color gamut data under an unknown illuminant for the optimization of the corrected matrix to decrease the computation time. In this case, the run-time of the optimization requires 3-5 min.

Several typical color constancy methods were selected as the comparison methods, namely, the Grey world (Buchsbaum, 1980), Shades of Grey (Finlayson and Trezzi, 2004), second-order Grey Edge (van de Weijer et al., 2007), SVR (Funt and Xiong, 2004), Generalized Gamut Mapping (Gijsenij et al., 2010), and Spatial Correlations (Chakrabarti et al., 2012).

Here some methods are use training set too. We set the training conditions according to the authors recommendation in the paper. As for SVR (Funt and Xiong, 2004), 3D data (chromaticity plus intensity) histogram is used. The radial basis kernel function is also chosen with the insensitivity parameter $\varepsilon = 0.00001$, punishment value $\eta = 0.1$, and shape parameter $\gamma = 0.025$. A training set of 45000 histograms from 6000 images is employed. As for Generalized Gamut Mapping (Gijsenij et al., 2010), the 1st-order data (i.e. edges) is used. The training set also has 6000 images from 15 different typical scenes. The standard deviation of the Gaussian smoothing filter is 3. As for Spatial Correlations (Chakrabarti et al., 2012), the maximum likelihood estimator is engaged. The training set also has 6000 images like that of Generalized Gamut Mapping.

Table 1: Angular errors for different color constancy methods on the SFU Grey-ball dataset.

Method	Mean	Median
Grey World	8.7°	8.4°
Shades of Grey	6.9°	6.4°
Second-order Grey Edge	6.3°	5.6°
SVR	7.0°	6.0°
Generalized Gamut Mapping	6.0°	4.7°
Spatial Correlations	5.4°	4.1°
Proposed Method	5.2°	3.3°

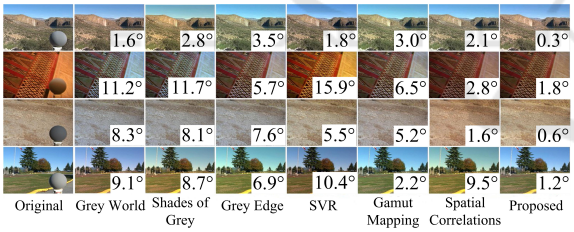

Figure 4: Sample comparison results of the SFU Grey-ball dataset. The angular error is listed on the grey ball.

Table 1 shows a comparison of the results. It indicates that our method is superior to the other methods. Some sample comparison results are shown in Fig. 4. Take the images in Fig. 4 for example, the influence of the number of images in training set is shown in Fig. 5. The correction performance enhances with more training images. About fifty images are required to obtain stable results.

4 CONCLUSIONS

We used the unsupervised kernel method, which is similar to the supervised learning method of SVR. For the image under an unknown illuminant, the corrected

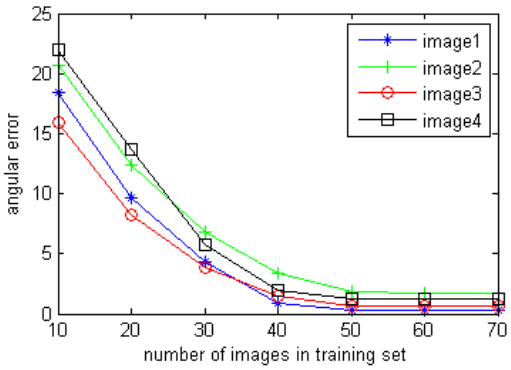

Figure 5: The angular error curve of the number of images in training set in fig. 4.

matrix is obtained by the optimization method. The optimized objective is that the corrected color data can satisfy the hyperplane of the canonical illuminant after being mapped to a high-dimensional space. After the correction, the sum of the distance from each point to the hyperplane has a minimum value. The test results on the SFU Grey-ball dataset show the effectiveness of the proposed method. The superiority of the proposed method is also supported by the analysis. The slice chart of the distance from the points in the RGB space to the hyperplane of the canonical illuminant shows that the method meets the grey world assumption. However, the proposed method differs from strong constraint methods, such as Grey World, which does not add these types of constraints to each scene. Therefore, better accuracy is achieved by this model, and a large area of monochromatic objects can be handled better.

The future work mainly focuses on two aspects. One is the computational efficiency. The run-time of the corrected matrix estimation requires several minutes. It limits the real-time application for digital imaging devices. Moreover, the training is also time consumed. The other aspect is the management of complex illumination environment. The ideal Lambertian model only deals with diffuse reflection. Although it is the most common cases, the specular reflection unavoidably appears in many scenes. Another complex illumination environment is multiple light source scenes. The effectiveness of the proposed approach could be influenced by these complex illumination, since its assumption is only the Lambertian model. The extension to the complex cases is another difficult but significant work.

ACKNOWLEDGEMENTS

This research was partially supported by National Natural Science Foundation (NSFC) of China under project No. 61403403 and First Class General Financal Grant of Chian Postdoctoral Science Foundation under project No.2015M52707.

REFERENCES

Barnard, K. (1999). *Dr. Thesis, Practical Color Constancy*. Simon Fraser University, Vancouver.

Bousetouane, F., Dib, L., and Snoussi, H. (2013). Improved mean shift integrating texture and color features for robust real time object tracking. *The Visual Computer*, 29(3):155–170.

Brainard, D. H. and Freeman, W. T. (1997). Bayesian color constancy. *Journal of the Optical Society of American A: Optics and Image Science, and Vision*, 14(7):1393–1411.

Buchsbaum, G. (1980). A spatial processor model for object color perception. *Journal of the Franklin Institute*, 310(1):337–350.

Cardei, V., Funt, B., and Barnard, K. (2002). Estimating the scene illumination chromaticity using a neural network. *Journal of the Optical Society of American A: Optics and Image Science, and Vision*, 19(12):2374–2386.

Chakrabarti, A., Hirakawa, K., and Zickler, T. (2008). Color constancy beyond bags of pixels. In *Computer Vision and Pattern Recognition*. IEEE.

Chakrabarti, A., Hirakawa, K., and Zickler, T. (2012). Color constancy with spatio-spectral statistics. *Pattern Analysis and Machine Intelligence, IEEE Transaction on*, 34(8):1509–1519.

Ciurea, F. and Funt, B. (2003). A large images database for color constancy research. In *11th Color Imaging Conference*, pages 160–164.

F.-H. Cheng, W.-H. H. and Chen, T.-W. (1998). Recovering colors in an image with chromatic illuminant. *Image Processing, IEEE Transactions on*, 7(11):1524–1533.

Finlayson, G., Drew, M., and Funt, B. (1993). Diagonal transforms suffice for color constancy. In *Int. Conf. Computer Vision*. IEEE.

Finlayson, G. and Trezzi, E. (2004). Shades of grey and color constancy. In *12th Color Imaging Conference*, pages :37–41.

Finlayson, G. D., Hordley, S. D., and Hubel, P. M. (2001). Color by correlation: A simple, unifying framework for color constancy. *Pattern Analysis and Machine Intelligence, IEEE Transaction on*, 23(11):1209–1221.

Forsyth, D. A. (1990). A novel algorithm for color constancy. *Int. J. Computer Vision*, 5:5–36.

Funt, B. and Xiong, W. (2004). Estimating illumination chromaticity via support vector regression. In *12th Color and Imaging Conference final program and Proceedings*, pages 47–52.

Gehler, P. V., Rother, C., Blake, A., Minka, T., and Sharp, T. (2008). Bayesian color constancy revisited. In *Computer Vision and Pattern Recognition*. IEEE.

Gijsenij, A. and Gevers, T. *Color constancy research website on illumination estimation*. http:// colorconstancy.com.

Gijsenij, A., Gevers, T., and Weijer, V. D. (2010). Generalized gamut mapping using image derivative structures for color constancy. *Int. J. Computer Vision*, 86(2-3):127–139.

Lai, S., Tan, X., Liu, Y., Wang, B., and Zhang, M. (2013). Fast and robust color constancy algorithm based on grey block-differencing hypothesis. *Optical review*, 20(4):341–347.

Land, E. (1977). The retinex theory of color vision. *Scientific American*, 237(6):108–128.

Pan, S. and Chen, J.-S. (2009). A damped gauss-newton method for the second-order cone complementarity problem. *Applied Mathematics and Optimization*, 59.

Rosenberg, C., Minka, T., and Ladsariya, A. (2004). Bayesian color constancy with non-gaussian models. In *In Advances in Neural Information Processing Systems (NIPS)*. Cambridge MA, MIT Press.

Stottinger, J., Hanbury, A., Sebe, N., and Gevers, T. (2012). Sparse color interest points for image retrieval and object categorization. *Image Processing, IEEE Transactions on*, 21(5):2681–2692.

Subramanian, P. K. (1993). Gauss-newton methods for the complementarity problem. *J. Optimization theory and applications*, 77(3).

van de Weijer, J., Gevers, T., and Gijsenij, A. (2007). Edge based color constancy. *Image Processing, IEEE Transactions on*, 16(9):2207–2214.

Zhuang, H., Low, K., and Yau, W. (2012). Multichannel pulse-coupled-neural-network-based color image segmentation for object detection. *Industrial electronics, IEEE Transactons on*, 59(8):3299–3308.